

Angular Triplet Loss-based Camera Network for ReID

Yitian Li

University of Electronic Science and Technology of China
Chengdu, China
liyitian1001@gmail.com

Ruini Xue

University of Electronic Science and Technology of China
Chengdu, China
xueruini@gmail.com

Mengmeng Zhu

University of Electronic Science and Technology of China
Chengdu, China
zmmeng96@163.com

Jing Xu

University of Electronic Science and Technology of China
Chengdu, China
xujing.may@gmail.com

Zenglin Xu

University of Electronic Science and Technology of China
Chengdu, China
zenglin@gmail.com

Abstract—Person re-identification (ReID) is a challenging cross-camera retrieval task to identify pedestrians. Many complex network structures are proposed recently and many of them concentrate on multi-branch features to achieve high performance. However, they are too heavy-weight to deploy in real-world applications. Additionally, pedestrian images are often captured by different surveillance cameras, so the varied lights, perspectives and resolutions result in inevitable multi-camera domain gaps for ReID. To address these issues, this paper proposes ATCN, a simple but effective angular triplet loss-based camera network, which is able to achieve compelling performance with only global features. In ATCN, a novel angular distance is introduced to learn a more discriminative feature representation in the embedding space. Meanwhile, a lightweight camera network is designed to transfer global features to more discriminative features. ATCN is designed to be simple and flexible so it can be easily deployed in practice. The experiment results on various benchmark datasets show that ATCN outperforms many SOTA approaches.

I. INTRODUCTION

Person re-identification (ReID) is a task of identifying bounding boxes of persons in the photos taken by multiple non-overlapping cameras. Given a query image, ReID needs to retrieve the images of the same identity in the gallery as the query one. That is, all images of the same person should be checked. For example, ReID has been widely adopted in monitoring, activity analysis, and people tracking [1], in which scenarios discriminative feature representation is critical. Therefore, the challenge of ReID is to learn a discriminative feature representation.

Due to the high discriminative ability of deep-learned representations, much significant progress of ReID has been made [2]–[11]. Lots of research considers ReID as a classification problem by taking the person IDs as different classes, and employs the typical softmax loss to learn a classification

hyperplane. It is the network before the classifier, *feature extractor*, responsible for feature representation learning [2]–[4], [8]. However, ReID is actually a ranking problem, and some leverage metric learning, such as triplet loss [15], to directly learn the feature representations [5]–[7]. The triplet loss tries to pull the features of one same identity closer and push away the ones of different identities. In contrast to softmax, triplet loss directly controls the learning process in embedding space, which is able to ensure features of the same identity are closer than others by a threshold margin. However, triplet loss is unstable due to its limited local optimization, making it hard to converge.

ReID images are usually captured by multi-cameras. Thus the inherent changing lights and perspectives will lead to inevitable camera-cased gaps in ReID datasets. To alleviate the gaps, [12] takes advantage of GAN to transfer images from one camera to another, and [13] transfers images from one dataset to another. However, it is too time-consuming for GAN to generate pedestrian images.

To address these challenges, this paper proposes a two-stage framework, ATCN, a ReID oriented Angular Triplet-based (AT) Camera Network (CN). ATCN adopts *angular-distance* as the distance metric of triplet loss, thus a linear decision boundary can be guaranteed, making it easier to combine with softmax loss in order to achieve local and global optimization at the same time. A new camera network is designed to address the problem of the camera-cased gaps, which consists of a feature transfer adapter and a camera discriminator. They play a minimax game: the camera discriminator tries to identify whether the feature is taken from specific cameras, while the adapter tries to transfer global features to fight against the discriminator. In this way, it can learn a pedestrian-discriminative-sensitive and multi-camera-

invariant feature representation.

Both AT and CN algorithms are straightforward and efficient, and they could be deployed independently or simultaneously. The prototype of ATCN is implemented with PyTorch [14] and is evaluated against two widely adopted ReID datasets. The experimental results show that either AT or CN outperforms the baseline as well as many existing methods, while the combination of them delivers the best results.

The main contributions of the paper are as follows:

- We propose AT for the feature-extract stage, which leverages “angle-distance” to ensure a linear decision boundary, outperforming conventional euclidean distance and cosine similarity.
- We propose CN for the feature-transfer stage to filter the camera information, ensuring the feature extractor can concentrate on the pedestrian information to bridge the gaps stemming from camera noises.
- By conducting extensive experiments on two widely used datasets, the results show that ATCN performs the best in contrast to many SOTA approaches.

II. RELATED WORK

A. Triplet loss

Triplet loss is introduced in FaceNet [15] for face recognition and clustering. Compared to softmax loss, who can take into account the global information and update the weights in each batch, so the entire training process is relatively smooth and stable. However, for triplet loss, the information involved and updated in each batch is very limited, therefore it’s prone to repeated training and is difficult to converge. Lots of sampling strategies are introduced to address this problem. For example, Song takes all pairwise distances in a batch to take full advantage of a batch [16], Chen adopts quadruplet loss with two negative samples for better generalization capability [5], Hermans proposes TriNet with PK -style sampling method and hardest example mining [9], and Ristani claims that most hard example mining methods only consider the hardest triplets or semi-hard triplets, but it can be beneficial to easy triplets as well [17]. Adaptive weights triplet loss providing high and low weights for hard and easy triplets are proposed as well.

B. ReID with Multi-branches features

ReID tasks usually encounter pose variance and occlusion problems, increasing the difficulty of ReID. There is lots of research on multi-branches features, such as pose-guided [18]–[20], mask-guided [21], [22] and stripe-based [2], [23] methods. All of them use “multiple local features”. Qi uses a forward mask to alleviate the problem of cluttered background and appearance variations [21], Kalayeh integrates human semantic parsing to harness local visual cues [22], and Wei leverages the local and global cues in human body to generate a discriminative and robust representation [18]. PoseBox structure [19] is devised to align pedestrians to a standard pose, while Sun provides a PCB network to learn several part-level features [2]. Dai uses two branches to provide a more comprehensive and spatially distributed feature representation, which consists of a

global branch and a drop branch, respectively [23]. Generally, the solutions of less features are regarded better if they could deliver no-worse results, because the models are simpler and various problems could be addressed only by generally applicable global features.

C. Multi-Camera ReID

ReID suffers from image style variations caused by differences in perspectives, surrounding and poses of multi-cameras. Zhong uses CycleGAN [24] to transfer images from one camera to another to bridge the gaps [12], and Wei proposes a Person Transfer Generative Adversarial Network which transfers images from a dataset to another to bridge the domain gap in different datasets [13]. Zhuang uses Camera-based Batch Normalization to force the image data to fall into the same subspace to shrink the distribution gap between any camera pair [25].

III. METHODOLOGY

A. Triplet Loss

Triplet loss [15] is one of the popular loss functions for metric learning. For a triplet (a, p, n) , triplet loss is formulated as (1):

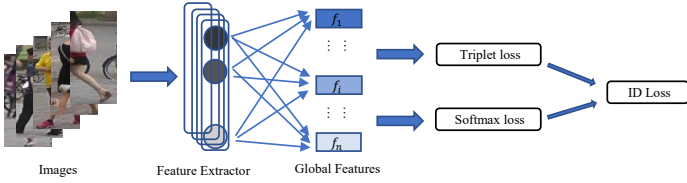
$$\mathcal{L}_{tri} = [D(f_{\theta}(a), f_{\theta}(p)) - D(f_{\theta}(a), f_{\theta}(n)) + m]_{+}, \quad (1)$$

where $D(x, y)$ is a metric function measuring distance or similarity between x and y in the embedding space \mathbb{R}^d , a denotes an anchor sample, p a positive sample with the same ID as a , and n a negative sample. f_{θ} is the feature extractor with parameter θ . For the sake of clarity, $D(x, y)$ will be used as a shortcut of $D(f_{\theta}(x), f_{\theta}(y))$, where $f_{\theta}(\cdot)$ is omitted. m the margin threshold that $D(a, p)$ must be less than $D(a, n)$ by at least m . The notation $[\cdot]_{+}$ means $\max(0, \cdot)$.

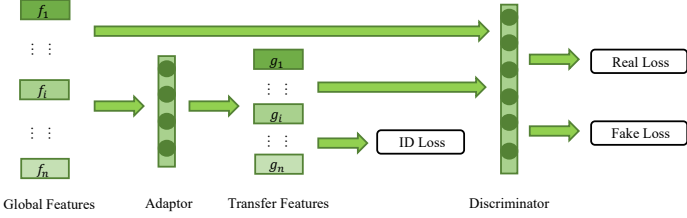
It can be recognized from the formula that triplet loss is designed to pull the positives closer and simultaneously push the negatives away with a threshold margin, aimed at $D(a, n) \geq D(a, p) + m$. Lots of ReID research [5], [15], [17], [26], [27] trains the model with triplet loss with $L2$ -norm distance as the distance metric function $D(x, y)$. Meanwhile, the sampling strategy Batch-Hard [9] is widely used as well, which picks P classes randomly, and then samples K images for each class to create $P \times K$ hardest positive and negative pairs, contributing to the triplet loss in a mini-batch.

B. Angular Triplet Loss

The fundamental challenge of ReID is encoding images into robust discriminative features. Triplet loss provides a detailed local optimization, which directly controls the process of learning embedding. However, as aforementioned in Section II-A, triplet loss’ local optimal constraint can not guarantee a global optimization because inter-class distance sometimes is smaller than the intra one. Therefore, we propose to combine softmax loss and triplet loss altogether to build more robust models, which are able to learn a more discriminative feature. As illustrated in Fig. 1(a), the images are extracted to global features, and two stream loss, *i.e.* triplet loss and softmax loss,



(a) The feature-extract stage.



(b) The feature-transfer stage.

Fig. 1. An overview of the proposed ATCN framework. In the feature-extract stage, ID loss leads the backbone model to learn a global feature representation. In the feature-transfer stage, camera discriminator takes both the global features and transfer features as input, then real loss and fake loss are computed, respectively. ID loss and negative fake loss lead feature adapter to learn more discriminative features.

are computed. All these processes are in the feature-extract stage to learn the feature extractor F .

Softmax loss is often used with a classifier, and enables the classifier to learn a global hyperplane for classification because it focuses on relative distance. However, triplet loss with $L2$ -norm distance reflects euclidean distances, so it does not make sense to combine them because of their inconsistent targets. Instead, cosine similarity as the distance metric function for triplet loss could make a more relaxed limit because its relative distance property aligns with softmax. The feature extractor will learn a linear hyperplane which is supposed to be better integrated with the classifier. By using cosine similarity as the distance metric function, the triplet loss could be formulated as (2):

$$\mathcal{L}_{cos} = [\cos(\theta_n) - \cos(\theta_p) + m]_+ \quad (2)$$

where θ_p and θ_n are the angles between (a, p) and (a, n) , respectively.

Although cosine similarity works well, in the later stage of training, positive samples and negative samples are basically distinguished, then small gradient will make it difficult to continue optimization. For example, when the angle between positive pairs is very small, the derivative of the angular distance is much larger than the derivative of the cosine similarity. To address this problem, we design \mathcal{L}_{ang} as in (3).

$$\mathcal{L}_{ang} = [\theta_p - \theta_n + m]_+ \quad (3)$$

\mathcal{L}_{ang} is different from \mathcal{L}_{cos} because the derivative of \mathcal{L}_{ang} is sharper by leveraging $\arccos(\cos(\theta)) = \theta$. Therefore, even if the features are distinguished, sufficient gradients can be guaranteed. The angular distance can achieve better results

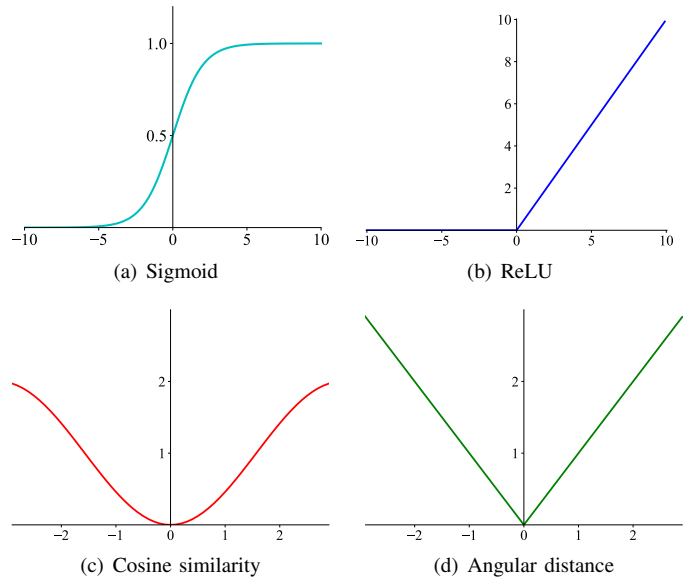


Fig. 2. The difference between cosine similarity and angular distance. The horizontal axis is the angle in radian measure.

than cosine similarity in both easy triplet and hard triplet cases because of the steeper curve, which is helpful for the convergence of the triple loss. Similar ideas can be found from the difference between ReLU [28] and Sigmoid. Fig.2 shows that the gradient of angular is steeper always. Note that $d(\arccos(x)) = -1/(\sqrt{1-x^2})dx$, so $\cos(\theta)$ is truncated from $\epsilon - 1$ to $1 - \epsilon$ to avoid the denominator to be 0, where ϵ is a very small scalar, and it is set $\epsilon = 10^{-7}$ in our experiments.

Given prediction logits p_k and label y_k of class k , the final loss called ID loss illustrated in (4), is the combination of triplet loss \mathcal{L}_{ang} and softmax loss \mathcal{L}_{soft} .

$$\begin{aligned} \mathcal{L}_{soft} &= \sum_{k=1}^K -y_k \log(p_k) \\ \mathcal{L}_{ID} &= \mathcal{L}_{ang} + \mathcal{L}_{soft} \end{aligned} \quad (4)$$

Actually, ReID can hardly be regarded as a typical classification problem, because the number of person IDs in the training set and test set might be completely different. It is more likely a one-shot learning task. For a classification task in this case, Label Smoothing [29] is a widely used method to avoid overfitting. Given a small constant α , the original label y_k will be smoothed to y_k^{LS} , as shown in (5).

$$y_k^{LS} = y_k(1 - \alpha) + \frac{\alpha}{K} \quad (5)$$

where K is the the number of classes, y_k is the indicator variable, α is a hyperparameter controlling the smoothness, and is set to 0.1 in the experiments. Label Smoothing can significantly improve the performance of the model.

C. Camera Network

As demonstrated in Section I, ReID images are usually taken by multi-cameras, causing differences in perspectives, surrounding and poses, making it hard to learn a robust

Algorithm 1 Pseudo code of the optimization.

Initialization: anchors: $\mathcal{A} = \{a_1, \dots, a_m\}$;
extracted features: $\mathcal{T} = \{t_1, \dots, t_m\}$;
labels: $\mathcal{Y} = \{y_1, \dots, y_m\}$;
hyperparameters: λ, μ ;

1: **repeat**

2: update θ_D by descending stochastic gradients:

3:

$$\theta_D \leftarrow \theta_D - \mu \cdot \nabla \theta_D \frac{1}{m} \mathcal{L}_D$$

4: update θ_F by descending stochastic gradients:

5:

$$\theta_T \leftarrow \theta_T - \lambda \cdot \nabla \theta_T \frac{1}{m} \mathcal{L}_T$$

6: **until** convergence

Output: learned features representations: $f_{\mathcal{T}}(\mathcal{T})$

model. The camera related noisy information is also encoded into the extracted features, which is harmful for person-ID identification. Therefore, the challenge is how to get rid of such camera information from feature representations. This is possible to accomplish by an adversarial network with a camera discriminator.

After feature-extract stage, the parameter θ_F is fixed, so F is used to extract global features only. As illustrated in Figure 1(b), the proposed Camera Network consists of a discriminator D and a adapter T , with parameter θ_D and θ_T , respectively. The responsibility of T is transferring global features f_i to more discriminative features g_i , and D tries to distinguish whether the current feature containing the information belongs to the cameras. The goal of D is to lead the learning process of T to get perspective-invariant features representations. Different from conventional adversarial network, *e.g.* GAN [30], which only contains real loss and fake loss, the loss function \mathcal{L}_T is combined with \mathcal{L}_{ID} to prevent feature adapter from losing the important person information learned by F . The loss function of D and F is shown as in (6):

$$\begin{aligned} \mathcal{L}_{real} &= -\log(D(f_i)) \\ \mathcal{L}_{fake} &= -\log(1 - D(T(f_i))) \\ \mathcal{L}_D &= \mathcal{L}_{real} + \mathcal{L}_{fake} \\ \mathcal{L}_T &= \mathcal{L}_{ID} - \mathcal{L}_{fake} \end{aligned} \quad (6)$$

where f_i is the the global feature extracted by F .

Optimization As shown in the formula \mathcal{L}_D and \mathcal{L}_T , the process of training T is to minimize \mathcal{L}_{ID} and maximize \mathcal{L}_{fake} at the same time. D learns to distinguish cameras by minimizing \mathcal{L}_D , which forms an adversarial relationship. Since the goals of the two objective functions are opposite, the training process of the minimax game can be divided into two sub-processes. One sub-process optimizes T , and the other optimizes D . Both the two sub-processes are implemented with Adam [31]. In our experiments, we train T and D alternatively, as shown in Algorithm 1.

TABLE I
REID DATASETS.

Dataset	ID	Box	Box/ID	Camera
Market1501	1,501	32,688	21.78	6
DukeMTMC	1,404	36,411	25.93	8

IV. EXPERIMENTS

A. Datasets

ATCN is evaluated against 2 widely used ReID datasets: Market1501 [32] and DukeMTMC [33]. The number of cameras and many other metrics vary across the datasets as illustrated in Table I. Market1501 contains 32,688 images of 1,501 person identities, captured by 6 cameras (5 high-resolution cameras, and 1 low-resolution camera). There are 751 identities for training and 750 for testing, 19,732 gallery images and 12,936 training images detected by DPM [34], and 3,368 manually cropped query images. DukeMTMC consists of 1,404 identities captured by 8 cameras. All the 36,411 bounding boxes are manually labeled. The evaluation protocol in [33] is adopted in our experiments: 16,522 images of 702 identities in the training set, 700 identities in the testing set, with 17,661 images in the gallery and 2,228 images for query.

B. Implementation

1) *Training Parameter:* The prototype of ATCN is implemented with Pytorch followed by a strong baseline [11]. All of the models are trained using a single NVIDIA Tesla V100. For a fair comparison, all experiments share the same global configuration. *PK*-style batch is employed to form a triplet data sampler. The batch size is set to 64, including 16 identities and 4 images for each identity. All images are resized to (256, 128). For data augmentation, random horizontal flips and random erasing augmentation [35] are adopted with the probability setting to 50%. Adam [31] is chosen as the optimizer for both feature extractor and camera network. For backbone F , the base learning rate is 3.5×10^{-4} with weight decay factor 5×10^{-4} . For discriminator D and adapter T , the base learning rate is 1.0×10^{-4} without weight decay. All other hyper-parameters of the optimizers are default in Pytorch.

2) *Network Architecture:* We follow a widely accepted open-source standard baseline, ResNet50 [36] with last stride 1 [2] is chosen as the feature extractor, and the pretrained weights provided by [36] is used. For the auxiliary network at the feature-transfer stage, a very lightweight network is designed for deployment efficiency and resource saving in practice. Discriminator D contains only 1 fully connected layer, and sigmoid function is applied after the fully connected layer. We use only 1 fully connected layer without bias, and the input channel is set to 2048 while the output channel 2048 for the feature adapter T . It is worth mentioning that the weight of T is initialized with the identity matrix, so that T retains the original features at the beginning of training.

TABLE II
INFLUENCE OF DIFFERENT TRICKS.

Method	Market1501		DukeMTMC	
	mAP	rank-1	mAP	rank-1
standard	66.9	83.5	57.5	75.2
+triplet [15]	71.9	86.7	62.9	76.9
+stride=1 [2]	72.6	86.3	62.9	78.0
+Warmup [37]	77.1	89.5	66.1	80.6
+LS [29]	78.6	90.4	67.8	82.5
+REA [35]	82.8	92.1	71.9	83.4
+BNNeck [11]	85.7	94.1	76.2	86.2

3) *Training Strategy*: At the feature-extract stage, the number of epochs is set to 120, and the learning rate will decay at 40 epochs and 70 epochs with a decay factor of 0.1, respectively. Additionally, warmup learning rate method [37] is applied. We use 10 epochs to linearly increasing the learning rate from 3.5^{-6} to 3.5^{-4} . At the feature-transfer stage, the number of epochs is set to 75 without learning rate decay. D and F are trained alternately, that is, one iteration for D and another for F . As a result, on Market1501, there are approximately 11,257 iterations ($1501/16 \times 120$) in feature-extract stage, and another 7,035 iterations ($1501/16 \times 75$) in the feature-transfer stage, resulting in a total of 18,292 iterations. It usually takes 1.5 hours for feature extractor training and another 0.5 hours for camera discriminator training in our configuration.

C. Evaluation

ReID is usually regarded as a ranking problem, so Mean average precision (mAP) score and cumulative matching curve (CMC) at rank-1 are reported in our results as most related research [5], [9], [38], [39]. Single query mode is used in all the experiments.

1) *Analysis of ATCN*: Compared with the standard baseline (only softmax is used), we additionally integrate triplet loss [15], last stride 1 [2], Warmup Learning Rate method [37], Label Smoothing [29], Random Erasing Augmentation [35] and BNNeck [11]. Although these training techniques are widely used, for a fair comparison, we still conduct a detailed analysis of these tricks before evaluating our methods. The results are shown in Table II. All of them are evaluated against Market1501 and DukeMTMC datasets. Backbone with last stride setting to 2 is regarded as the standard baseline, and the results of other tricks are reported from top to bottom in stacking. For example, “+triplet” means that triplet loss is added to the standard baseline model. The results indicate that even for Euclidean distance, “+triplet” can bring remarkable improvement due to its local optimization. By applying all the tricks, Market1501 could reach 18.8% and 10.6% improvement for mAP and CMC rank-1, respectively, while for DukeMTMC, they are 18.7% and 11%, respectively.

Then, the combination of all tricks (last line in Table II) is consider as the baseline in Table III, and AT (only changes Euclidean distance to the proposed angular distance), CN (only apply camera network) and ATCN are applied incrementally.

TABLE III
EVALUATION OF ATCN.

Method	Market1501		DukeMTMC	
	mAP	rank-1	mAP	rank-1
Baseline	85.7	94.1	76.2	86.2
AT	86.3	94.4	76.8	86.8
CN	86.9	94.2	76.6	86.9
ATCN	86.9	94.5	77.1	87.9

TABLE IV
COMPARISON WITH SOTA METHODS.

Method	N_f	Market1501		DukeMTMC	
		mAP	rank-1	mAP	rank-1
PN-GAN [8]	9	72.6	89.4	53.2	73.6
MaskReID [21]	5	75.3	90.0	61.9	78.8
GLAD [18]	4	73.9	89.9	-	-
PCB [2]	6	81.6	93.8	69.2	83.3
SPReID [22]	5	81.3	92.5	71.0	84.4
BDB [23]	2	84.3	94.2	72.1	86.8
Pyramid [10]	21	88.2	95.7	79.0	89.0
SVDNet [40]	1	62.1	82.3	56.8	76.7
TriNet [9]	1	69.1	84.9	-	-
TriNet+Era [35]	1	-	-	56.6	73.0
CamStyle [12]	1	68.7	88.1	53.5	75.3
AWTL [17]	1	75.7	89.5	63.4	78.9
DuATM [41]	1	76.6	91.4	62.3	81.2
Pyramid [10]	1	82.1	92.8	-	-
BDB [23]	1	80.6	93.1	-	-
AT	1	86.3	94.4	76.8	86.8
CN	1	86.9	94.2	76.6	86.9
ATCN	1	86.9	94.5	77.1	87.9

ATCN increases mAP from 76.2% to 77.1%, and rank-1 accuracy from 86.4% to 87.9% on DukeMTMC, and delivers 0.7% and 0.6% improvement for mAP and rank-1 accuracy on Market1501, respectively. Since we only use the global feature and all improvement is based on a very strong baseline, ATCN performs very well indeed.

2) *Comparison with SOTA methods*: ATCN is also evaluated against some SOTA methods, and the results are reported in Table IV. The methods are classified into two categories according to the number of features, N_f . ATCN outperforms many current methods on Market1501 and DukeMTMC, particularly compared with those only use 1 feature. Pyramid [10] achieves an excellent score using 21-branches features, but ATCN beats it by 4.8% and 1.7% with only 1 feature. It can be observed that ATCN outperforms all the methods that use 1 feature. On all the two datasets, both AT and CN can achieve competitive performance, while ATCN usually get the best scores, which is a strong implication that both AT and CN are helpful to learn pedestrian-discriminative-sensitive and multi-camera-invariant representations and the combination of them ATCN could leverage them simultaneously.

TABLE V
COMPARISON OF DIFFERENT DISTANCE METRICS.

Metric	Market1501		DukeMTMC	
	mAP	rank-1	mAP	rank-1
Euclidean	85.6	93.8	76.1	86.2
Cosine	86.2	93.9	76.2	86.4
Angular	86.3	94.4	76.8	86.8



Fig. 3. 4 images selected from Market1501. The first two are the same person captured by different cameras, while the last two are different people.

3) *Comparison of distance metrics*: As metric learning, the distance metric function is very important for triplet loss. Lots of research is devoted to design distance metric functions suitable for ReID, and the most popular ones are Euclidean distance and cosine distance. Since different distance metric functions can affect the results significantly, it is necessary to evaluate how this is related to ATCN. Therefore, we evaluate Euclidean distance, cosine distance and angular distance, and the results are presented in Table V. For ReID datasets, angular distance used in ATCN could deliver better outcomes because it can learn a more discriminative feature representation.

In order to demonstrate how different distance metrics work for a specific person query, we select 4 images from Market1501, two of which are the same person while the other two are not. For the sake of clarity, the image is named as “P i -C j ”, while i is the person ID and j the camera ID. As illustrated in Figure 3, P595-C6 is selected as the query image, and P595-C3 (the same person), P693-C4 and P1203-C5 are selected as gallery images. Table VI presents the Euclidean and angular distances for different gallery images. It is clear that the angular distance can cluster the features of the same person and separate the features of different people better.

4) *Comparison of model training*: We compare ATCN with other publically available models as in Table VII. ATCN requires less memory and can finish training more quickly than the other models. PN-GAN [8] needs to train a GAN network for pose conversion, while SPReID [22] needs a semantic segmentation network and pretrained Inception-V3 weight to segment the images, both of which undoubtedly increase the cost.

V. CONCLUSION

To achieve better performance and address multi-camera gap challenges in ReID applications, this paper proposed ATCN, an angular triplet loss-based camera network. AT performs beyond the Euclidean distance and cosine similarity based triplet loss functions on various datasets. For domain

TABLE VI
THE DISTANCE BETWEEN A PAIR OF QUERY AND GALLERY IMAGES.

Metric	P595-C3	P693-C4	P1203-C5
Euclidean	0.705	1.115	2.048
Angular	0.674	1.317	2.108

TABLE VII
COMPARISON OF MODEL TRAINING.

Method	Memory usage (GB)	Training time (min)
PCB [2]	7.52	156
BDB [23]	15.49	207
ATCN	6.33	109

gaps introduced by multi-cameras, CN is devised to filter useless multi-camera information, which transfers features to pedestrian-discriminative-sensitive and multi-camera-invariant feature representations. The model is more robust to tolerate the noise from different cameras. Though AT and CN are targeted to ReID initially, they could be ported and implemented to other domain applications, especially triplet loss related use cases. In the future, we will improve the camera network in terms of structure and training strategy.

REFERENCES

- [1] Chen, B., Deng, W., Hu, J.: Mixed high-order attention network for person re-identification. In: Proceedings of the IEEE International Conference on Computer Vision. (2019) 371–381
- [2] Sun, Y., Zheng, L., Yang, Y., Tian, Q., Wang, S.: Beyond part models: Person retrieval with refined part pooling (and a strong convolutional baseline). In: Proceedings of the European Conference on Computer Vision (ECCV). (2018) 480–496
- [3] Li, D., Chen, X., Zhang, Z., Huang, K.: Learning deep context-aware features over body and latent parts for person re-identification. In: Proceedings of the IEEE Conference on Computer Vision and Pattern Recognition. (2017) 384–393
- [4] Zhao, H., Tian, M., Sun, S., Shao, J., Yan, J., Yi, S., Wang, X., Tang, X.: Spindle net: Person re-identification with human body region guided feature decomposition and fusion. In: Proceedings of the IEEE Conference on Computer Vision and Pattern Recognition. (2017) 1077–1085
- [5] Chen, W., Chen, X., Zhang, J., Huang, K.: Beyond triplet loss: a deep quadruplet network for person re-identification. In: Proceedings of the IEEE Conference on Computer Vision and Pattern Recognition. (2017) 403–412
- [6] Cheng, D., Gong, Y., Zhou, S., Wang, J., Zheng, N.: Person re-identification by multi-channel parts-based cnn with improved triplet loss function. In: Proceedings of the IEEE conference on computer vision and pattern recognition. (2016) 1335–1344
- [7] Xiao, Q., Luo, H., Zhang, C.: Margin sample mining loss: A deep learning based method for person re-identification. arXiv preprint arXiv:1710.00478 (2017)
- [8] Qian, X., Fu, Y., Xiang, T., Wang, W., Qiu, J., Wu, Y., Jiang, Y.G., Xue, X.: Pose-normalized image generation for person re-identification. In: Proceedings of the European conference on computer vision (ECCV). (2018) 650–667
- [9] Hermans, A., Beyer, L., Leibe, B.: In defense of the triplet loss for person re-identification. arXiv preprint arXiv:1703.07737 (2017)
- [10] Zheng, F., Deng, C., Sun, X., Jiang, X., Guo, X., Yu, Z., Huang, F., Ji, R.: Pyramidal person re-identification via multi-loss dynamic training. In: Proceedings of the IEEE Conference on Computer Vision and Pattern Recognition. (2019) 8514–8522

- [11] Luo, H., Gu, Y., Liao, X., Lai, S., Jiang, W.: Bag of tricks and a strong baseline for deep person re-identification. In: Proceedings of the IEEE Conference on Computer Vision and Pattern Recognition Workshops. (2019) 0–0
- [12] Zhong, Z., Zheng, L., Zheng, Z., Li, S., Yang, Y.: Camera style adaptation for person re-identification. In: The IEEE Conference on Computer Vision and Pattern Recognition (CVPR). (June 2018)
- [13] Wei, L., Zhang, S., Gao, W., Tian, Q.: Person transfer gan to bridge domain gap for person re-identification. In: Proceedings of the IEEE conference on computer vision and pattern recognition. (2018) 79–88
- [14] Paszke, A., Gross, S., Chintala, S., Chanan, G., Yang, E., DeVito, Z., Lin, Z., Desmaison, A., Antiga, L., Lerer, A.: Automatic differentiation in pytorch (2017)
- [15] Schroff, F., Kalenichenko, D., Philbin, J.: Facenet: A unified embedding for face recognition and clustering. In: Proceedings of the IEEE conference on computer vision and pattern recognition. (2015) 815–823
- [16] Oh Song, H., Xiang, Y., Jegelka, S., Savarese, S.: Deep metric learning via lifted structured feature embedding. In: Proceedings of the IEEE Conference on Computer Vision and Pattern Recognition. (2016) 4004–4012
- [17] Ristani, E., Tomasi, C.: Features for multi-target multi-camera tracking and re-identification. In: Proceedings of the IEEE conference on computer vision and pattern recognition. (2018) 6036–6046
- [18] Wei, L., Zhang, S., Yao, H., Gao, W., Tian, Q.: Glad: Global-local-alignment descriptor for pedestrian retrieval. In: Proceedings of the 25th ACM international conference on Multimedia. (2017) 420–428
- [19] Zheng, L., Huang, Y., Lu, H., Yang, Y.: Pose-invariant embedding for deep person re-identification. *IEEE Transactions on Image Processing* **28**(9) (2019) 4500–4509
- [20] Saquib Sarfraz, M., Schumann, A., Eberle, A., Stiefelwagen, R.: A pose-sensitive embedding for person re-identification with expanded cross neighborhood re-ranking. In: Proceedings of the IEEE Conference on Computer Vision and Pattern Recognition. (2018) 420–429
- [21] Qi, L., Huo, J., Wang, L., Shi, Y., Gao, Y.: Maskreid: A mask based deep ranking neural network for person re-identification. arXiv preprint arXiv:1804.03864 (2018)
- [22] Kalayeh, M.M., Basaran, E., Gökmen, M., Kamasak, M.E., Shah, M.: Human semantic parsing for person re-identification. In: Proceedings of the IEEE Conference on Computer Vision and Pattern Recognition. (2018) 1062–1071
- [23] Dai, Z., Chen, M., Gu, X., Zhu, S., Tan, P.: Batch dropblock network for person re-identification and beyond. In: Proceedings of the IEEE International Conference on Computer Vision. (2019) 3691–3701
- [24] Zhu, J.Y., Park, T., Isola, P., Efros, A.A.: Unpaired image-to-image translation using cycle-consistent adversarial networks. In: Proceedings of the IEEE international conference on computer vision. (2017) 2223–2232
- [25] Zhuang, Z., Wei, L., Xie, L., Zhang, T., Zhang, H., Wu, H., Ai, H., Tian, Q.: Rethinking the distribution gap of person re-identification with camera-based batch normalization. In: European Conference on Computer Vision, Springer (2020) 140–157
- [26] Ding, S., Lin, L., Wang, G., Chao, H.: Deep feature learning with relative distance comparison for person re-identification. *Pattern Recognition* **48**(10) (2015) 2993–3003
- [27] Sohn, K.: Improved deep metric learning with multi-class n-pair loss objective. In: Advances in Neural Information Processing Systems. (2016) 1857–1865
- [28] Glorot, X., Bordes, A., Bengio, Y.: Deep sparse rectifier neural networks. In: Proceedings of the fourteenth international conference on artificial intelligence and statistics. (2011) 315–323
- [29] Zheng, Z., Zheng, L., Yang, Y.: A discriminatively learned cnn embedding for person reidentification. *ACM Transactions on Multimedia Computing, Communications, and Applications (TOMM)* **14**(1) (2017) 1–20
- [30] Goodfellow, I., Pouget-Abadie, J., Mirza, M., Xu, B., Warde-Farley, D., Ozair, S., Courville, A., Bengio, Y.: Generative adversarial nets. In: Advances in neural information processing systems. (2014) 2672–2680
- [31] Kingma, D.P., Ba, J.: Adam: A method for stochastic optimization. arXiv preprint arXiv:1412.6980 (2014)
- [32] Zheng, L., Shen, L., Tian, L., Wang, S., Wang, J., Tian, Q.: Scalable person re-identification: A benchmark. In: Computer Vision, IEEE International Conference on. (2015)
- [33] Zheng, Z., Zheng, L., Yang, Y.: Unlabeled samples generated by gan improve the person re-identification baseline in vitro. In: The IEEE International Conference on Computer Vision (ICCV). (Oct 2017)
- [34] Felzenszwalb, P., McAllester, D., Ramanan, D.: A discriminatively trained, multiscale, deformable part model. In: 2008 IEEE Conference on Computer Vision and Pattern Recognition, IEEE (2008) 1–8
- [35] Zhong, Z., Zheng, L., Kang, G., Li, S., Yang, Y.: Random erasing data augmentation. arXiv preprint arXiv:1708.04896 (2017)
- [36] He, K., Zhang, X., Ren, S., Sun, J.: Deep residual learning for image recognition. In: Proceedings of the IEEE conference on computer vision and pattern recognition. (2016) 770–778
- [37] Fan, X., Jiang, W., Luo, H., Fei, M.: Spherereid: Deep hypersphere manifold embedding for person re-identification. *Journal of Visual Communication and Image Representation* **60** (2019) 51–58
- [38] Zhong, Z., Zheng, L., Cao, D., Li, S.: Re-ranking person re-identification with k-reciprocal encoding. In: Proceedings of the IEEE Conference on Computer Vision and Pattern Recognition. (2017) 1318–1327
- [39] Wang, B., Yang, Y., Xu, X., Hanjalic, A., Shen, H.T.: Adversarial cross-modal retrieval. In: Proceedings of the 25th ACM international conference on Multimedia, ACM (2017) 154–162
- [40] Sun, Y., Zheng, L., Deng, W., Wang, S.: Svdnet for pedestrian retrieval. In: Proceedings of the IEEE International Conference on Computer Vision. (2017) 3800–3808
- [41] Si, J., Zhang, H., Li, C.G., Kuen, J., Kong, X., Kot, A.C., Wang, G.: Dual attention matching network for context-aware feature sequence based person re-identification. In: Proceedings of the IEEE Conference on Computer Vision and Pattern Recognition. (2018) 5363–5372